Warm Non-Equilibrium Plasma-Assisted Catalysis for Sustainable Ammonia Synthesis – Supplementary Information

Ananthanarasimhan Jayanarasimhan[a], Abhishek Umesh Shetty[a], Dinesh Dhanabal[a,1], Sharanya Acharya[a,1], KVSS Bhargavi[a], Reetesh Kumar Gangwar[b], Debayan Saha[a,c], Shashi Ranjan*[a,c]

[a]Faraday Earth Private Limited, Bengaluru 560001, India
[b]Department of Physics & CAMOST, Indian Institute of Technology Tirupati, Yerpudu 517619, India
[c]Faraday Earth Incorporation, Wilmington, Delaware 19808, United States

[1]Authors contributed equally
*Corresponding author (shashi@faradayearth.com)

S1. RGA-assisted catalysis for NH_3 synthesis - Experimental setup & operating conditions

Ammonia synthesis was investigated in a two-stage setup comprising a RGA plasma reactor for non-thermal activation of feed gas, followed by a downstream post plasma catalytic zone. Figure S1 shows the schematic of the experimental setup. A N_2/H_2 mixture was sent to the RGA reactor through two tangential inlets, at a total flow rate of 3.01 SLPM, controlled using the mass flow controller (M/s Alicat Scientific). An AC kHz high voltage power supply was used to power the conical high voltage electrode. The stainless-steel metal body was grounded. Post-plasma catalytic chamber has a triangular cross-section, partially filled with catalyst pellets and the catalyst bed was positioned at the start of the diverging zone, to interact with the plasma plume (as seen in Figure S1). All the Glass, Fe, Cu and Ni were cylindrical pellets with similar geometry (3 mm diameter, 4 ± 1 mm length). The catalyst bed zone was filled with appropriate number of pellets, accounting the fact that slight variation in pellet dimension will affect the pressure across the catalyst bed and porosity. Catalyst pellets were packed at the bottom 2.4 cm (24 mm) height, starting from the narrow gas inlet to ensure immediate contact with plasma-activated species (see Figure S1). The calculation of porosity and gas residence time was done considering the pellet volume, and the residence time was corrected accordingly. Catalyst bed volume was 6480 mm^3. Void fraction was calculated using the expression,

$$\varepsilon = \frac{(bed\ volume - total\ solid\ volume)}{bed\ volume}$$

and the gas residence time was calculated using the expression,

$$residence\ time\ (\tau) = \frac{Packed\ bed\ volume(mL) \times mean\ porosity}{volumetric\ flow\ rate\ \left(\frac{mL}{s}\right)}$$

The plasma plug power was monitored using a commonly used power monitor/power meter [1], kept constant to $\approx 170.0 \pm 3.0$ W. The NH_3 was quantified at the outlet of catalyst chamber under ambient temperature condition, using Uniphos ammonia gas detector with a calibrated 100 ml sampling pump provided by Uniphos. The ammonia was also trapped in acidified water and quantified using colorimetric technique, explained in detail in the following subsection.

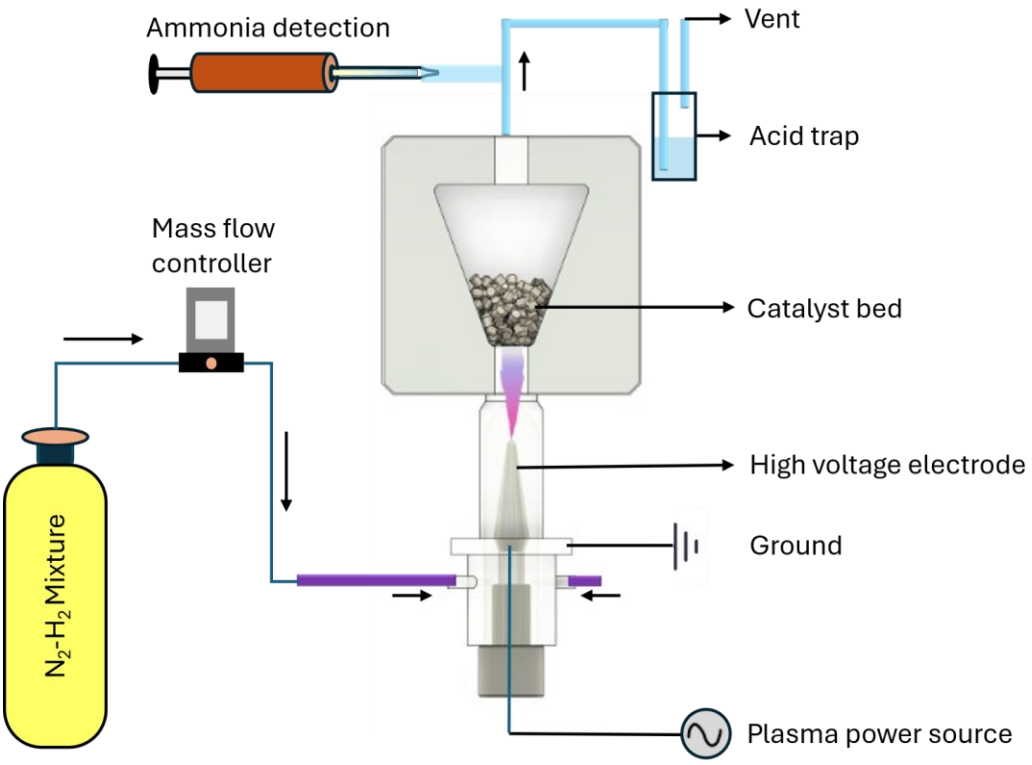

Figure S1. Schematic of the experimental setup of RGA-assisted catalysis for ammonia synthesis.

S1.1 Quantification of ammonia using acid trap-colorimetric technique

Ammonia quantification was performed using an acid trap followed by the colorimetric indophenol blue method [2,3]. The post-plasma effluent gas (3.01 LPM) was bubbled through 200 mL of 0.05 M H_2SO_4 for five minutes to capture gaseous NH_3 as aqueous ammonium. For colorimetric analysis, a 2 mL aliquot of this analyte was mixed with the following reagent mixture:

- Solution A (1.6 mL): 1 M NaOH containing 5 wt.% salicylic acid and 5 wt.% trisodium citrate dihydrate.
- Solution B (400 µL): 0.05 M sodium hypochlorite.
- Solution C (120 µL): 1 wt.% sodium nitroprusside.

Following a one-hour incubation in the dark, the absorbance of the solution was measured at 655 nm via UV-vis spectrophotometry. Ammonium concentrations were determined against a standard calibration curve (0.05–2 ppm NH_4^+ in 0.05 M H_2SO_4; Figure S2), with samples diluted as needed to remain within the calibration limits. The final outlet ammonia gas concentration was subsequently derived from the aqueous concentration and trapping constants using the expression: $[NH_3]_{gas} = \frac{[NH_4^+]_{analyte}}{0.05548}$.

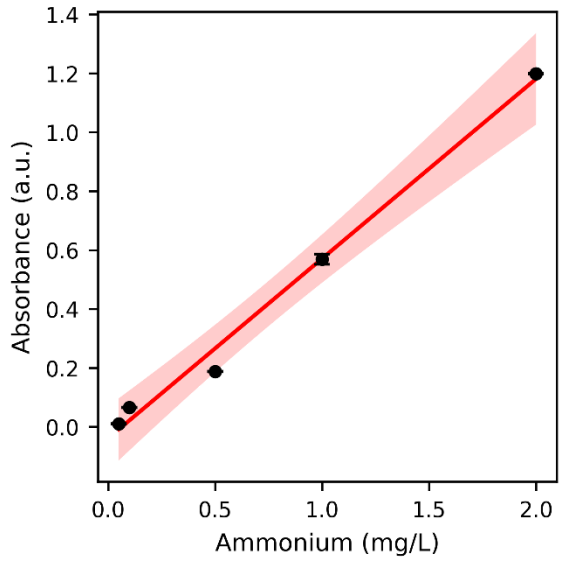

Figure S2. Calibration curve for the colorimetric quantification of ammonium ions. The solid line represents the linear regression fit of the experimental absorbance data (black circles). Error bars represent the standard deviation of the calibration standards. The shaded region illustrates the 95% confidence interval of the regression line, strictly bound within the tested concentration range (0.05 to 2.0 mg/L). The resulting linear fit equation is "$Absorbance = (0.61 \times Ammonium) - 0.0389$" with an R-squared value of 0.99. The propagated standard error of prediction is calculated using $Error(Ammonium) = 0.08823 \cdot \sqrt{\frac{1}{m} + \frac{1}{5} + \frac{(Ammonium - 0.73)^2}{2.598}}$, where m is the number of experimental replicates.

S2. Energy-dispersive X-ray spectroscopy (EDS) characterization of Fe, Ni and Cu pellets

Energy-dispersive X-ray spectroscopy (EDS) was employed to examine the elemental composition and phase purity of the Fe, Ni and Cu pellets. Figure S3 shows the EDS spectra acquired from the selected areas exhibit characteristic L and K emissions lines corresponding exclusively to Fe, Ni and Cu, respectively. Quantitative analysis using the eZAF correction method reveals that each analyzed region consists of 100 wt % and 100 at. % of the respective elements, with no secondary elements detected.

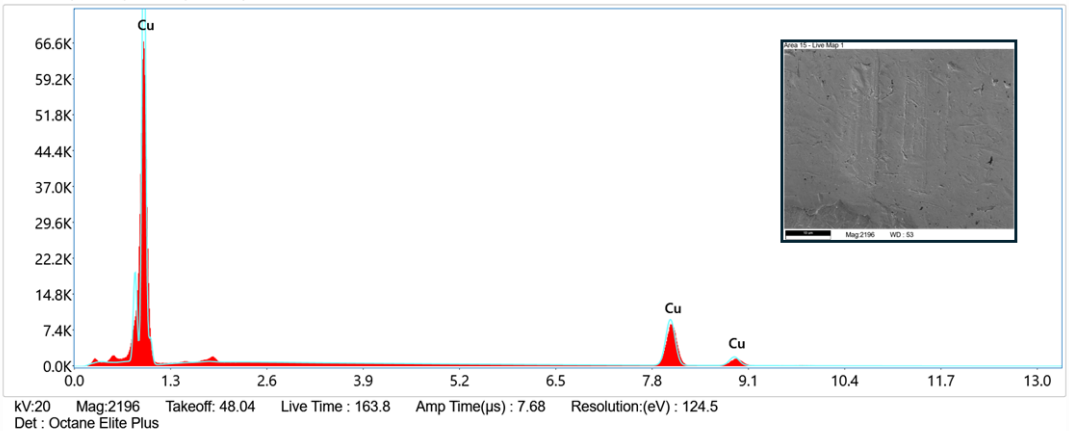

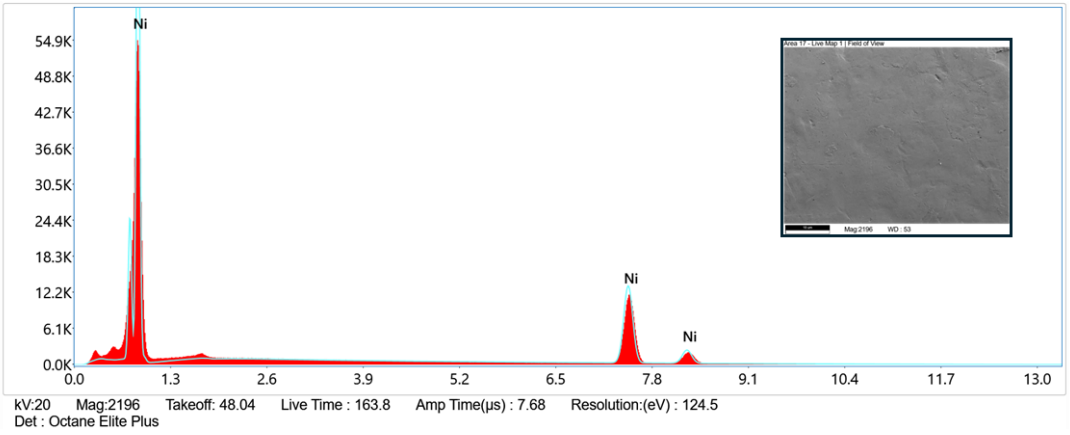

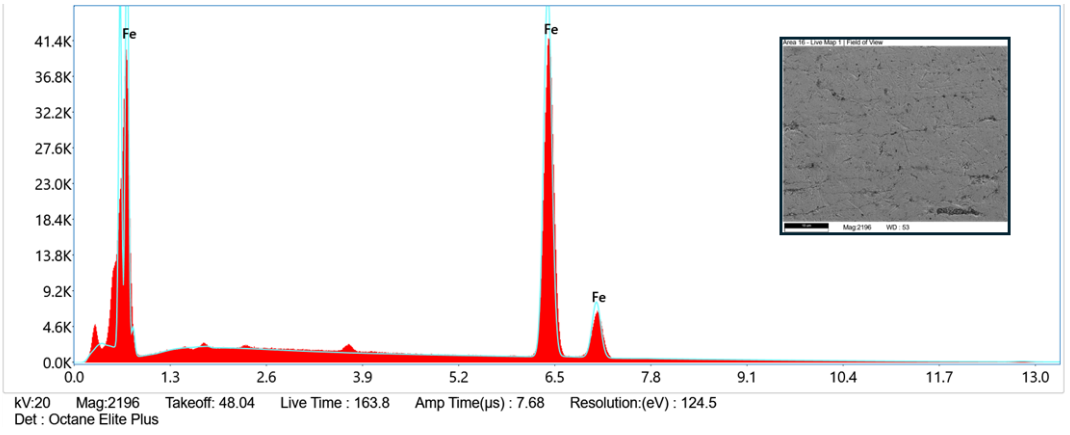

Figure S3. EDS spectra of the selected areas of Cu, Ni and Fe pellets (from top to bottom); inset shows the selected area for the characterization.

S3. Details of vibrational temperature of RGA

Spectra of nitrogen plasma from the RGA reactor of this work were collected (see figure S4) using Ocean Optics HDX spectrometer (slit 10 μm) coupled with a 1000 μm optic fiber. The vibrational temperature (T_{vib}) was determined from the emission of the N_2's second positive system in the 300-400 nm range, using the mean spectrum obtained by repeating data collection thrice. Following the methodology of Biloiu et al. [4], T_{vib} was calculated from the relative intensities of the vibrational bands (specifically the $\Delta v = -2$ sequence). These lower-lying states are expected to be nearly thermalized via rapid $v - v$ exchange in this atmospheric-pressure RGA; this is justified by the excellent linearity of the Boltzmann plot in figure S5(a). The measured T_{vib} was 0.29 eV $\approx$ 0.3 eV. As shown in figure S5(b), the fractional population of levels above 5 is negligible. The use of a Boltzmann distribution for this estimation is valid as the populations of first few vibrational levels are nearly identical in both Boltzmann and non-equilibrium (e.g., Treanor) distributions [5]; this is verified and shown in Figure S6 where in the Boltzmann distribution for T_{vib} of 0.3 eV (this work) is compared with Treanor distribution for the same T_{vib}, corresponding to gas temperatures 1000 K and 1500 K (typical range for RGA kinds of plasmas); for all the cases, 99% of the vibrational population is below the level 6.

It must be noted that the vibrational distribution is of the electronically excited $C^3\Pi_u$ state ($T_{vib,C}$), rather than the ground state (T_{vib}) that primarily drives the catalytic surface reactions. Equating $T_{vib,C}$ to T_{vib} in non-equilibrium plasmas introduces inherent uncertainties, as the ground state Vibrational Distribution Function (VDF) can differ from the excited states [6]. To address this, we draw upon the rigorous analysis by Dilecce et al. [6]. Their work demonstrates that for the pressure, gas temperature, and electronic temperature ranges typical of RGAs, the relative populations of the lowest C-state levels ($v \leq 1$) are almost insensitive to changes in the T_{vib} , with sensitivity only emerging at $v \geq 2$.

- Crucially, approximately 93% of the observed population in our measurements resides strictly in those $v \leq 2$ levels.
- Furthermore, as described in the previous paragraph, the vibrational distribution was obtained by capturing the $\Delta v = -2$ sequence of SPS, which consists of emissions from the lowest excited levels ($v' = 0,1,2,3$).

For these reasons, and because the assumption of a Boltzmann distribution remains largely valid for the lowest vibrational levels irrespective of the electronic state, $T_{vib,C}$ serves as a highly reliable first-order proxy for tracking the relative vibrational excitation of the plasma. Therefore, while equating the absolute values of $T_{vib,C}$ to T_{vib} directly remains a key macroscopic assumption, it serves as a robust proxy that does not alter the derived Volcano plot or the fundamental conclusions of this study.

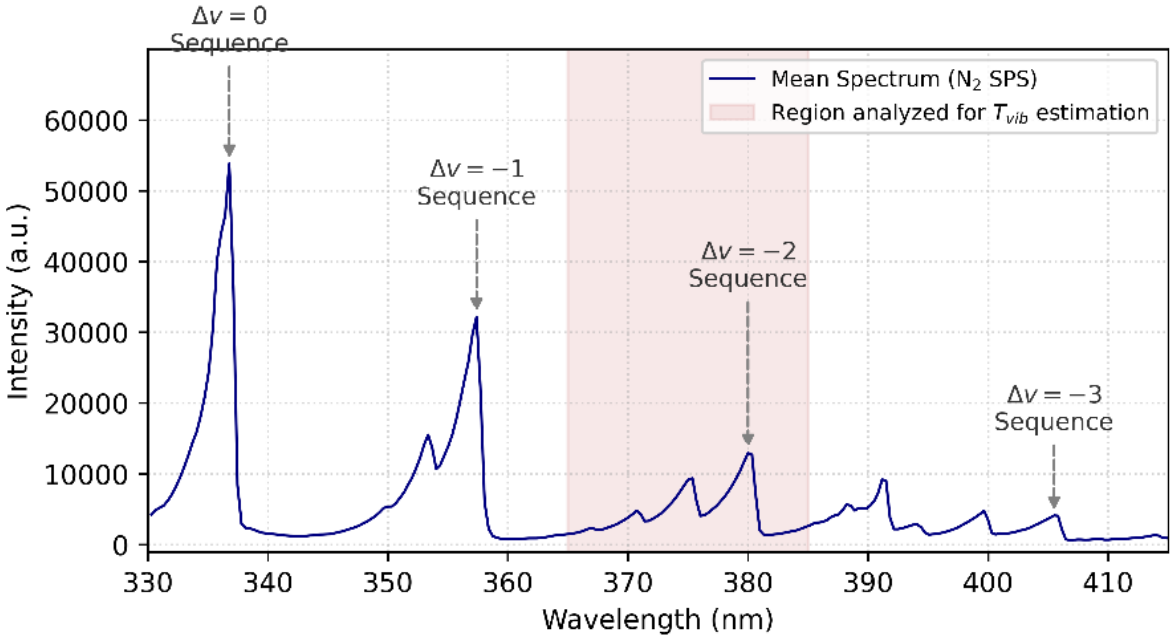

Figure S4. OES spectrum of the RGA showing nitrogen second positive system (SPS), indicating the region considered for obtaining vibrational temperature using Boltzmann plot (see Figure S4(a)).

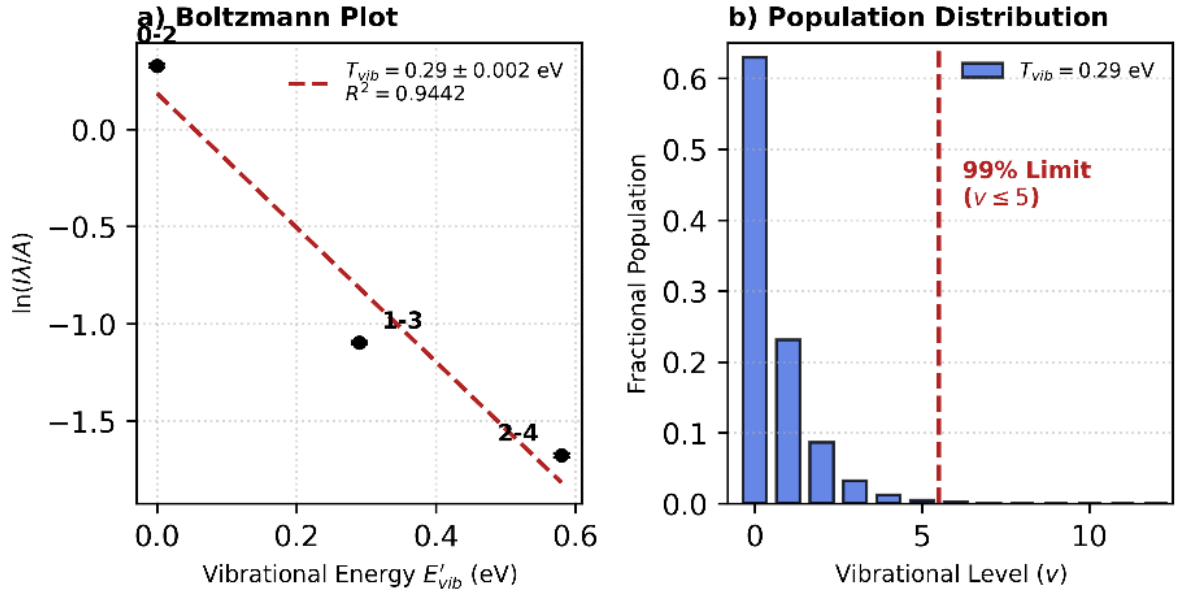

Figure S5. (a) Boltzmann fit of the N_2 second positive system indicating a mean vibrational temperature of 0.29 eV. (b) Calculated population using Boltzmann distribution indicating 99% of the population is below level 6.

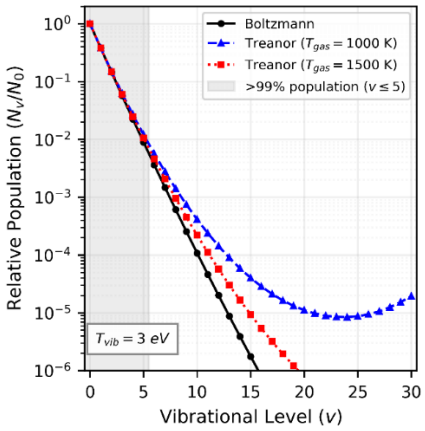

Figure S6. Vibrational distribution function (VDF) of N_2 across varying conditions. Comparison of the relative vibrational population (N_v/N_0) for a Boltzmann distribution at the experimentally determined $T_{vib} = 0.3$ eV (~3481 K) and Treanor distributions for the same $T_{vib} = 0.3$ eV at representative gas temperatures ($T_{gas} = 1000$ K and 1500 K). The shaded grey region denotes the 99% Vibrational Population Zone ($v \leq 5$), containing the vast majority of the molecular density. While the Treanor model accounts for anharmonic V-V "up-pumping" into the high-energy tail ($v > 8$), the distribution within the shaded grey region remains effectively indistinguishable from a Boltzmann distribution. This visual and mathematical overlap justifies the use of a Boltzmann-weighted descriptor for the plasma-catalytic volcano plot, as the kinetic rate is driven by the primary energy manifold ($v \leq 5$) which remains independent of T_{gas} fluctuations.

References

1. Jaiswal, A. K., Ananthanarasimhan, J., Shivapuji, A. M., Dasappa, S. & Rao, L. Experimental investigation of a non-catalytic cold plasma water-gas shift reaction. *J. Phys. D: Appl. Phys.* **53**, 465205 (2020).

2. Searle, P. L. The berthelot or indophenol reaction and its use in the analytical chemistry of nitrogen. A review. *Analyst* **109**, 549 (1984).

3. Dhanabal, D., Markandaraj, S. S. & Shanmugam, S. Transition Metal Nanoparticle-Embedded Nitrogen-Doped Carbon Nanorods as an Efficient Electrocatalyst for Selective Electroreduction of Nitric Oxide to Ammonia. *ACS Catal.* **13**, 9136–9149 (2023).

4. Biloiu, C., Sun, X., Harvey, Z. & Scime, E. Determination of rotational and vibrational temperatures of a nitrogen helicon plasma. *Review of Scientific Instruments* **77**, 10F117 (2006).

5. Mehta, P. *et al.* Overcoming ammonia synthesis scaling relations with plasma-enabled catalysis. *Nat Catal* **1**, 269–275 (2018).

6. Dilecce, G., Ambrico, P. F., Martini, L. M. & Tosi, P. On the determination of the vibrational temperature by optical emission spectroscopy. *Plasma Sources Sci. Technol.* **31**, 077001 (2022).